

**DESIGN AND OPTIMIZATION OF TRANSITION  
FOR AIR-FILLED SUBSTRATE INTEGRATED  
WAVEGUIDE**

**NUR HIDAYAH MANSOR**

**UNIVERSITI SAINS MALAYSIA**

**2018**

**DESIGN AND OPTIMIZATION OF TRANSITION FOR AIR-FILLED  
SUBSTRATE INTEGRATED WAVEGUIDE**

**by**

**NUR HIDAYAH BT MANSOR**

**Thesis submitted in fulfilment of the  
requirements for the degree of  
Doctor of Philosophy**

**April 2018**

## **ACKNOWLEDGEMENT**

All praise be to Allah, for His blessings and guidance for giving me the inspiration to complete this thesis and instilling in me the strength to see that this thesis becomes a reality. First, I would like to thank the Ministry of Higher Education (MOHE) and Universiti Sains Malaysia (USM) for giving me financial support without which I am unable to pursue a study. Second, I wish to deliver my deepest appreciation and gratitude to my supervisor Dr.-Ing Muhammad Razi Abdul Rahman for all his coaching, knowledge, encouragement, guidance and patience as well as moral supports without any hesitation which enable me to complete this thesis. I would also want to thank my second supervisor Dr. Aftarnasar Md. Shahar for sharing his knowledge and information. Above all, my whole-hearted thanks and appreciation to my beloved husband, mother, and siblings for their endless love, patience, financial support, and believe in me as well as moral supports throughout my journey to complete my Ph.D thesis. Not forgetting my late father and grandmother who always motivate me to get the high-level study. This thesis is dedicated to them.

## TABLE OF CONTENTS

	<b>Page</b>
<b>ACKNOWLEDGEMENT</b>	ii
<b>TABLE OF CONTENTS</b>	iii
<b>LIST OF TABLES</b>	vi
<b>LIST OF FIGURES</b>	viii
<b>LIST OF ABBREVIATIONS</b>	xi
<b>LIST OF SYMBOLS</b>	xiii
<b>ABSTRAK</b>	xv
<b>ABSTRACT</b>	xvii
<b>CHAPTER ONE: INTRODUCTION</b>	
1.1 Background	1
1.2 Problem Statement	4
1.3 Research Objectives	5
1.4 Scope and Limitation	6
1.5 Thesis Outline	6
<b>CHAPTER TWO: LITERATURE REVIEW</b>	
2.1 Inhomogeneous Waveguide	8
2.2 Air-Filled Substrate Integrated Waveguide	10
2.2.1 Air-filled SIW Structures	16
2.2.2 Dielectric- to Air-Filled SIW Transition	17
2.3 Optimization Procedure	19
2.3.1 Single-objective Genetic Algorithm	22

2.3.2	Multi-objective Genetic Algorithm	23
2.3.3	Clamped Cubic Spline Method	25
2.4	Summary	27

### **CHAPTER THREE: THEORETICAL ANALYSIS OF ELECTROMAGNETIC WAVE IN INHOMOGENEOUS WAVEGUIDE**

3.1	Derivation of Wave Equations	28
3.2	Inhomogeneous Waveguide	29
3.2.1	Dielectric Loaded Waveguide	30
3.2.2	Dielectric- to Air-Filled SIW Transition	33
3.2.3	Summary of Full-Wave Analysis Theory	36
3.3	Summary	38

### **CHAPTER FOUR: METHODOLOGY**

4.1	Design Specification of Air-filled SIW Transition	39
4.2	Design Parameters of Air-filled SIW Transition Structure	40
4.3	Full-wave Analysis of Air-Filled SIW Transition	44
4.3.1	Effect of Transition Length on Losses	45
4.3.2	Effect of Transition Taper Function on Losses	46
4.4	Project Implementation Flow	48
4.5	Optimization Procedure of Air-Filled SIW Transition	49
4.5.1	Construction of the transition taper with spline	49
4.5.2	Interface between ANSYS HFSS and MATLAB for optimization	53
4.5.3	Optimization of the results obtained from ANSYS HFSS using GA	53

4.5.4	Reconstruction of the transition taper for an optimization of length	55
4.6	Summary	57
<b>CHAPTER FIVE: RESULTS AND DISCUSSION</b>		
5.1	Full-wave Analysis of Dielectric- to Air- Filled SIW Transition	58
5.1.1	Effect of Transition Length on Losses	61
5.1.2	Effect of Transition Taper Function on Losses	64
5.2	Optimization of Air-Filled SIW Transition	70
5.3	Ka-band frequency	71
5.3.1	5 mm transition length	71
5.3.2	10 mm transition length	74
5.3.3	15 mm transition length	77
5.3.4	20 mm transition length	79
5.4	U-band frequency	83
5.4.1	5 mm transition length	83
5.4.2	10 mm transition length	85
5.4.3	15 mm transition length	87
5.4.4	20 mm transition length	89
5.5	Summary of Optimization Findings	92
<b>CHAPTER SIX: CONCLUSIONS</b>		
6.1	Summary	94
6.2	Contribution of Work	96
6.3	Future Work	96
<b>REFERENCES</b>		98
<b>LIST OF PUBLICATIONS</b>		

## LIST OF TABLES

		<b>Page</b>
Table 4.1	Structural Parameters	43
Table 4.2	Equation for Taper	47
Table 5.1	Optimized parameters obtained using MO optimization for 5 mm at Ka-band	72
Table 5.2	Optimized parameters obtained using MO optimization for 10 mm at Ka-band	75
Table 5.3	Optimized parameters obtained using MO optimization for 15 mm at Ka-band	77
Table 5.4	Optimized parameters obtained using MO optimization for 20 mm at Ka-band	79
Table 5.5	Percentage for return loss improvement of the optimized design compared to the RC-taper design.	82
Table 5.6	Percentage for insertion loss improvement of the optimized design compared to the RC-taper design.	83
Table 5.7	Optimized parameters obtained using MO optimization for 5 mm at U-band	83
Table 5.8	Optimized parameters obtained using MO optimization for 10 mm at U-band	85
Table 5.9	Optimized parameters obtained using MO optimization for 15 mm at U-band	87
Table 5.10	Optimized parameters obtained using MO optimization for 20 mm at U-band	89
Table 5.11	Percentage for return loss improvement of the optimized design compared to the RC-taper design.	91
Table 5.12	Percentage for insertion loss improvement of the optimized design compared to the RC-taper design.	92

## LIST OF FIGURES

		<b>Page</b>
Figure 1.1	Air-filled SIW transition. (Parment et al., 2015)	3
Figure 2.1	SIW: a) metalized via holes arrays b) metalized grooves. (Deslandes and Wu 2001)	11
Figure 2.2	Schematic and geometry of SIW. (Ng Mou Kehn, 2014)	12
Figure 2.3	SIW. ( Bozzi et al., 2009)	12
Figure 2.4	Half-mode SIW. (Lai et al., 2009)	14
Figure 2.5	Modified SIW. (Ranjesh and Shahabadi 2008)	15
Figure 2.6	Air-filled SIW. (Parment et al., 2015)	15
Figure 2.7	Air-filled SIW transition. (Parment et al., 2015)	17
Figure 3.1	Dielectric loaded waveguide. (Collins, 2001)	31
Figure 3.2	Dielectric loaded waveguide	31
Figure 3.3	Air-filled SIW transition. (Parment et al., 2014)	34
Figure 3.4	Meshed air-filled SIW transition	37
Figure 4.1	Air-filled SIW transition	41
Figure 4.2	Design of the transition taper in HFSS	45
Figure 4.3	Equation functions of taper	47
Figure 4.4	The steps of simulation	48
Figure 4.5	Clamped cubic spline profile of transition taper design	52
Figure 4.6	Flowchart of GA optimization with full-wave analysis for the fitness function	56
Figure 5.1	Configuration of air-filled SIW a) without the transition b) with the transition	58
Figure 5.2	Simulated $ S_{11} $ for an air filled SIW in Ka-band frequency: AFSIW-T = air filled SIW with the transition, AFSIW-NT = air filled SIW without the transition	59



Figure 5.3	Simulated $ S_{21} $ for an air filled SIW in Ka-band frequency: AFSIW-T = air filled SIW with the transition, AFSIW-NT = air filled SIW without the transition	59
Figure 5.4	The reflection coefficient $S_{11}$ results for different transition lengths	61
Figure 5.5	The transmission coefficient $S_{21}$ results for different transition lengths	64
Figure 5.6	Simulated $ S_{11} $ for a different transition shape of taper in Ka-band frequency at 33 GHz: L = linear equation, P = parabolic equation, E= exponential equation and RC = raised cosine equation at Ka-band	65
Figure 5.7	Simulated $ S_{11} $ for a different transition shape of taper in U-band frequency at 50 GHz: L = linear equation, P = parabolic equation, E = exponential equation and RC = raised cosine equation	66
Figure 5.8	Simulated $ S_{21} $ for a different transition shape of taper in Ka-band frequency at 50 GHz: L= linear equation, P = parabolic equation, E= exponential equation and RC = raised cosine equation	67
Figure 5.9	Simulated $ S_{21} $ for a different transition shape of taper in U-band frequency at 50 GHz: L = linear equation, P = parabolic equation, E = exponential equation and RC = raised cosine equation	67
Figure 5.10	Simulated $S_{11}$ for different transition lengths in Ka-band (Parment et al., 2015).	68
Figure 5.11	Simulated $S_{21}$ for different transition lengths in Ka-band (Parment et al., 2015).	69
Figure 5.12	Taper geometry with a clamped cubic spline for $L = 5$ mm.	72
Figure 5.13	Comparison of the optimized $ S_{11} $ between MO and SO method in Ka-band frequency at 33 GHz: RC = Raised Cosine, SO = Single-objective Genetic Algorithm, MO = Multi-objective Genetic Algorithm, AY= Arbitrary method.	73
Figure 5.14	Comparison of the optimized $ S_{21} $ between MO and SO method in Ka-band frequency at 33 GHz: RC = Raised Cosine, SO = Single-objective Genetic Algorithm, MO = Multi-objective Genetic Algorithm, AY= Arbitrary method.	73
Figure 5.15	Taper geometry with a clamped cubic spline for $L = 10$ mm.	75

Figure 5.16	Comparison of the optimized $ S_{11} $ between MO and SO method in Ka-band frequency at 33 GHz: RC = Raised Cosine, SO = Single-objective Genetic Algorithm, MO = Multi-objective Genetic Algorithm	75
Figure 5.17	Comparison of the optimized $ S_{21} $ between MO and SO method in Ka-band frequency at 33 GHz: RC = Raised Cosine, SO = Single-objective Genetic Algorithm, MO = Multi-objective Genetic Algorithm	76
Figure 5.18	Taper geometry with a clamped cubic spline for $L = 15$ mm.	77
Figure 5.19	Comparison of the optimized $ S_{11} $ between MO and SO method in Ka-band frequency at 33 GHz: RC = Raised Cosine, SO = Single-objective Genetic Algorithm, MO = Multi-objective Genetic Algorithm	78
Figure 5.20	Comparison of the optimized $ S_{21} $ between MO and SO method in Ka-band frequency at 33 GHz: RC = Raised Cosine, SO = Single-objective Genetic Algorithm, MO = Multi-objective Genetic Algorithm	78
Figure 5.21	Taper geometry with a clamped cubic spline for $L = 20$ mm.	80
Figure 5.22	Comparison of the optimized $ S_{11} $ between MO and SO method in Ka-band frequency at 33 GHz: RC = Raised Cosine, SO = Single-objective Genetic Algorithm, MO = Multi-objective Genetic Algorithm	80
Figure 5.23	Comparison of the optimized $ S_{21} $ between MO and SO method in Ka-band frequency at 33 GHz: RC=Raised Cosine, SO= Single-objective Genetic Algorithm, MO= Multi-objective Genetic Algorithm	81
Figure 5.24	Comparison of the optimized $ S_{11} $ between MO and SO method in U-band frequency at 50 GHz: RC = Raised Cosine, SO = Single-objective Genetic Algorithm, MO = Multi-objective Genetic Algorithm	84
Figure 5.25	Comparison of the optimized $ S_{21} $ between MO and SO method in U-band frequency at 50 GHz: RC = Raised Cosine, SO = Single-objective Genetic Algorithm, MO = Multi-objective Genetic Algorithm	84
Figure 5.26	Comparison of the optimized $ S_{11} $ between MO and SO method in U-band frequency at 50 GHz: RC = Raised Cosine, SO = Single-objective Genetic Algorithm, MO = Multi-objective Genetic Algorithm	86

Figure 5.27	Comparison of the optimized $ S_{21} $ between MO and SO method in U-band frequency at 50 GHz: RC = Raised Cosine, SO = Single-objective Genetic Algorithm, MO-GA= Multi-objective Genetic Algorithm	86
Figure 5.28	Comparison of the optimized $ S_{11} $ between MO and SO method in U-band frequency at 50 GHz: RC = Raised Cosine, SO = Single-objective Genetic Algorithm, MO = Multi-objective Genetic Algorithm	88
Figure 5.29	Comparison of the optimized $ S_{21} $ between MO and SO method in U-band frequency at 50 GHz: RC = Raised Cosine, SO=Single-objective Genetic Algorithm, MO = Multi-objective Genetic Algorithm	88
Figure 5.30	Comparison of the optimized $ S_{11} $ between MO and SO method in U-band frequency at 50 GHz: RC = Raised Cosine, SO = Single-objectives Genetic Algorithm, MO = Multi-objective Genetic Algorithm optimization	90
Figure 5.31	Comparison of the optimized $ S_{21} $ between MO and SO method in U-band frequency at 50 GHz: RC = Raised Cosine, SO = Single-objective Genetic Algorithm, MO = Multi-objective Genetic Algorithm	90
Figure 5.32	Percentage bandwidth of the return loss for Ka-band and U-band frequencies	92
Figure 5.33	Transmission loss of Ka-band and U-band frequencies at different percentage bandwidth	93

## LIST OF ABBREVIATIONS

<b>SIW</b>	Substrate Integrated Waveguide
<b>PCB</b>	Printed Circuit Board
<b>CBCPW</b>	Conductor-Backed Coplanar Waveguide
<b>HMSIW</b>	Half-Mode Substrate Integrated Waveguide
<b>HSIW</b>	Hollow Substrate Integrated Waveguide
<b>ESIW</b>	Empty Substrate Integrated Waveguide
<b>AFSIW</b>	Air-Filled Substrate Integrated Waveguide
<b>DFW</b>	Dielectric-Filled Waveguide
<b>TE</b>	Transverse Electric
<b>SIC</b>	Substrate Integrated Circuit
<b>GA</b>	Genetic Algorithm
<b>NPGA</b>	Niched Pareto GA
<b>NSGA</b>	Non-Dominated Sorting GA
<b>SPEA</b>	Strength Pareto Evolutionary Algorithm
<b>NSGA-II</b>	Elitist Non-Dominated Sorting Genetic Algorithm
<b>LSE</b>	Longitudinal Section Electric
<b>LSM</b>	Longitudinal Section Magnetic
<b>VBS</b>	Visual Basic Script
<b>AFSIW-NT</b>	Air-Filled SIW Without Transition
<b>AFSIW-T</b>	Air-Filled SIW With Transition
<b>RC</b>	Raised Cosine

<b>SO</b>	Single-objective Genetic Algorithm
<b>MO</b>	Multi-objective Genetic Algorithm
<b>L</b>	Linear Equation
<b>P</b>	Parabolic Equation
<b>E</b>	Exponential Equation

## LIST OF SYMBOLS

<b>E</b>	Electric field intensity vector
<b>H</b>	Magnetic field intensity vector
<b>D</b>	Electric flux density
<b>B</b>	Magnetic flux density vector
<b>J</b>	Current density vector
$\rho$	Charge density
$\epsilon$	Permittivity
$\mu$	Permeability
$\sigma$	Electric conductivity
$r$	Position vector
$\epsilon_r$	Substrate permittivity
$f_c$	Cut-off frequency
$c$	Velocity of light
$h_i$	Spacing between the points
$d_i$	The slopes
dB	Magnitude or logarithmic based decibels
GHz	Gigahertz
$k$	Wavenumber
$S_{11}$	Reflection coefficients
$S_{21}$	Transmission coefficient
V	Volts

m	Meter
A	Amperes
As	Amperes in one second
Vs	Volt in one second

# **REKABENTUK DAN PENGOPTIMUMAN PERALIHAN BAGI PANDU GELOMBANG BERSEPADU SUBSTRAT BERISI UDARA.**

## **ABSTRAK**

Pandu gelombang bersepadu substrat berisi udara adalah satu bentuk talian penghantaran baru yang telah digunakan untuk disambungkan dengan litar pandu gelombang bersepadu substrat untuk mengurangkan kehilangan penghantaran dan pantulan gelombang dalam litar. Untuk penyambungan yang berkesan, pelbagai cadangan bentuk peralihan antara media berisi udara dan dielektrik didalam pandu gelombang bersepadu substrat telah diberikan. Untuk meningkatkan prestasi peralihan, kehilangan penghantaran dan pantulan gelombang sepanjang peralihan mesti dikurangkan. Walau bagaimanapun, kehilangan gelombang dalam peralihan tidak difahami dengan baik. Ini di sebabkan perambatan gelombang elektromagnet di sepanjang media yang berbeza dengan pelbagai geometri adalah sukar untuk dikenal pasti. Tesis ini membentangkan kajian mendalam untuk mencirikan perambatan gelombang dan kehilangan gelombang dalam peralihan dengan melakukan analisis gelombang penuh. Hasil daripada penaksiran geometri peralihan berisi udara kepada dielektrik, prosedur pengoptimuman telah dibangunkan untuk meminimumkan kehilangan gelombang dalam struktur. Penentuan bentuk tirus peralihan dengan kaedah gelugur kabus, menunjukkan bahawa kehilangan gelombang selanjutnya boleh dikurangkan di dalam jalur gelombang frekuensi seperti Ka-band (26-40 GHz) dan U-band (40-60 GHz). Tambahan pula, panjang tirus peralihan juga boleh dikurangkan dengan ketara di samping mengekalkan kualiti optimum penghantaran isyarat dalam peralihan. Dengan mengoptimumkan geometri peralihan, isyarat dalam bentuk gelombang elektromagnet akan melalui peralihan dengan kehilangan penghantaran dan pantulan gelombang yang minimum.



Kaedah kajian berangka dalam kes-kes spesifik pengoptimuman peralihan menunjukkan penambah baikkkan sebanyak 45% kehilangan pantulan gelombang di dalam frekuensi Ka-band dan 48.3% di dalam frekuensi U-band. Manakala, penambah-baikkkan dalam kehilangan penghantaran gelombang sebanyak 3.1% di dalam Ka-band dan 4.0% di dalam U-band telah di peroleh. Penemuan kajian ini menyumbang kepada pembangunan reka bentuk litar sesatah yang lebih padat untuk pelbagai jalur frekuensi dengan prestasi yang lebih baik.

# **DESIGN AND OPTIMIZATION OF TRANSITION FOR AIR-FILLED SUBSTRATE INTEGRATED WAVEGUIDE**

## **ABSTRACT**

Air-filled substrate integrated waveguide (SIW) is a new form of transmission lines that have been used as interconnect with conventional SIW circuits to reduce losses in the circuits. For an effective interconnection, various proposals for the transition between the air-filled and dielectric-filled media in SIW have been given. To increase the performance of the transition, the insertion and return losses along the transition must be minimized. However, the losses in the transition are not well understood. This is because the propagation of electromagnetic waves along the inhomogeneous media with varying geometry is difficult to characterize with respect to losses. This thesis presents an in-depth study to characterize the propagation of the waves and losses in the transition using full-wave analysis. From the assessment of the transition geometry from air-filled to dielectric-filled SIW, an optimization procedure is developed to further minimize the losses in the structure. Defining the shape of the transition taper with the cubic clamped spline function, the developed procedure shows that further reduction of losses is possible within the prescribed frequency bands, i.e., Ka-band (26-40 GHz) and U-band (40-60 GHz). Furthermore, the length of the transition taper can also be significantly reduced while maintaining an optimal quality of signal transmission in the transition. Hence, by optimizing the transition geometry, the signal in the form of electromagnetic waves will pass through the transition with minimal return loss and insertion loss. The numerical studies in specific cases of the transition optimization show an improvement of 45% return loss at Ka-band frequencies and 48.3% return loss at U-band frequencies. Meanwhile, the improvements of transmission loss by 3.1% at Ka-band and 4.0% at

U-band were obtained. The findings of the present study will contribute to the development of a more compact design of coplanar circuits for any frequency bands with better performance.

# CHAPTER ONE

## INTRODUCTION

### 1.1 Background

Growing interest in developing high-quality microwave and millimeter wave integrated circuits and systems sees substrate integrated waveguide (SIW) as a promising component in printed circuit substrate technologies. The advantages of SIW are it provides a compact, light, flexible, low-cost and mass-productive alternative to the conventional bulky waveguide and planar Printed Circuit Board (PCB) transmission lines including microstrip or Conductor-Backed Coplanar Waveguide (CBCPW).

The SIW structures also maintain most of the advantages of conventional metallic waveguides such as high quality-factor and high power-handling capability (Che et al., 2008). Moreover, SIW technology enables to fabricate a complete circuit including planar circuitry, transitions, rectangular waveguides, active components and antennas in planar form, using a standard printed circuit board or other planar processing techniques (Bozzi et al., 2009).

As a consequent, various components based on the SIW technology have been proposed and applied in the past years for operation in the microwave and mm-wave range, including filters, couplers, oscillators, slot-array antennas, six-port circuits, circulators and etc. However, one of the major issues in the design of SIW components is related to the minimization of losses, especially when operating in the mm-wave frequency range (Bozzi et al., 2009). The mechanisms of loss in the SIW

structures consist of conductor losses due to the finite conductivity of metallic walls, radiation losses due to the presence of gaps in the SIW structures along the side walls and lastly dielectric losses due to the loss tangent of the dielectric substrate (Bozzi et al., 2008). According to Bozzi et al. (2009), the dielectric loss is typically the most significant contribution to losses in the mm-wave frequency range.

Hence a significant effort has been devoted to the research and development of low loss SIW components. The earliest design developed to reduce the dielectric loss in SIW structure is the half-mode substrate integrated waveguide (HMSIW) proposed by Lai et al. (2009) where the waveguide width and the surface area of the metallic sheets are reduced by nearly half.

Later on, a new design of SIW structure has been attempted by removing the central dielectric region of an SIW with the intention of achieving a much lower loss. For an example, modified SIW with an air cut region by Ranjkesh and Shahabadi (2006), hollow substrate integrated waveguide (HSIW) by Jin et al. (2014), the empty substrate integrated waveguide (ESIW) by Belenguer et al. (2014), and an air-filled substrate integrated waveguide (AFSIW) by Parment et al. (2015).

To allow an effective interconnect, the transition from the dielectric-filled toward an air-filled SIW circuit has been proposed in Parment et al. (2015). As a wave propagates between two different media, part of the wave, in general, is reflected while another part is transmitted into the second medium (Kraus and Fleisch, 1999). This mechanism is referred to as reflection and transmission loss. According to Ghassami et al. (2014), the development of a wideband transition of the transmission line on different dielectric constant substrates becomes critical for complete front-end integration and low-cost system manufacturing.

To evaluate the performance of an air-filled SIW circuit, the transition from the dielectric substrate toward the hollow, i.e., the air-filled region must be properly characterized (Parment et al., 2015). However, a systematic and comprehensive study to characterize the influence of the dielectric-air transition on losses in an air-filled SIW is still lacking to date. This thesis assesses the influence of the transition taper geometry in the complete SIW structure in which the transition tapers are mathematically described with various geometrical functions such as linear, parabolic, exponential, and raised cosine function as part of the solution of the characteristic function. In addition, an optimization procedure is developed to re-design the transition geometry in order to further minimize the losses along the transition.

The transition taper as depicted in Figure 1.1 is penetrating from the air into the dielectric material when seen from right to left. For that reason, air-filled SIW transition is more complex as an inhomogeneous rectangular waveguide. Therefore, theoretical analysis of inhomogeneous waveguide is applied to analyze air-filled SIW structure losses.

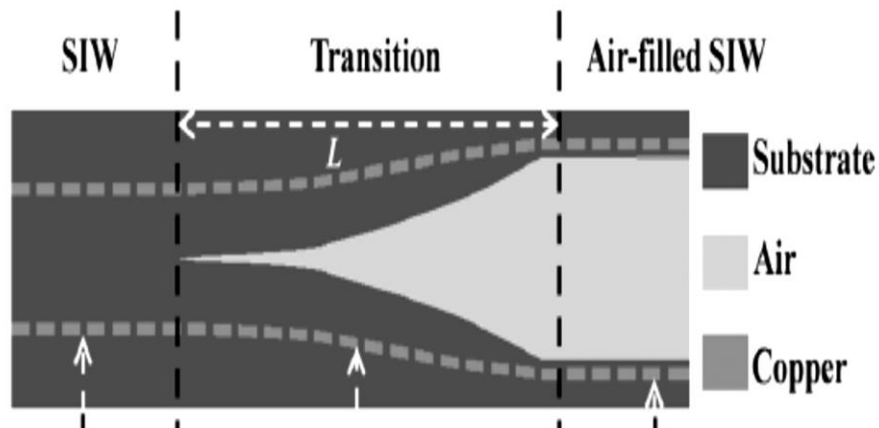


Figure 1.1: Air-filled SIW transition (Parment et al., 2015).

The propagation characteristics and the field modes associated with the electromagnetic waves that propagate inside the structures must satisfy the source-free Maxwell's equations. Different from the uniform waveguide, the analysis of the electromagnetic waves inside the inhomogeneous waveguide is quite challenging. This is because, when the guide is loaded with two or more dielectric materials, the solution becomes difficult to handle due to the involved transcendental equations which occur for the determination of the eigenvalues such as the propagation constant and the mode fields (Collins, 1960). Alternatively, the full-wave analysis by using the high-frequency structural simulator (ANSYS HFSS) has been applied to analysis an air-filled SIW transition structure.

## **1.2 Problem Statement**

To increase the performance of an air-filled SIW in terms of losses, the insertion and return losses along the dielectric- to air-filled transition needed to be characterized. In addition, various proposals for the transition of an air-filled SIW on air- to dielectric-filled media must be proposed in order to minimize the losses. In order to characterize the losses, the electromagnetic field and propagation constant of an electromagnetic wave along the transition structure need to be considered. However, the propagation constant of electromagnetic waves along the inhomogeneous media with varying geometry is difficult to calculate. The primary reason is that the closed-form expressions for the propagation constants of complex geometry are impossible to determine. In addition, the approach of the equivalent microwave circuit is also not guaranteed to yield a reliable eigenvalue equation, which is used to investigate the loss of transition structure. As a result, the losses in

the transition are still not well understood. Therefore, the losses along the transition cannot be determined. Furthermore, the optimization of an air-filled SIW transition design cannot be done because of the return and transmission losses are used as the objective functions in an optimization method.

### **1.3 Research Objectives**

The first goal of this thesis is to understand the return and transmission losses along the transition in an air-filled SIW in order to completely characterize the losses in an air-filled SIW complete structure. From the understanding, the performance of an air-filled SIW transition can be systematically improved. Then, the second goal is to optimize losses in an air-filled SIW complete structure. To fulfill the goals, there are five objectives to be achieved as follows:

1. To analyze the electromagnetic waves and losses along the dielectric-to air-filled SIW transition.
2. To evaluate the effects of the transition taper geometry on the dielectric- to air-filled SIW transition losses.
3. To develop an optimization procedure using the multi-objective genetic algorithm.
4. To design the transition taper geometry using clamped cubic spline functions.
5. To validate the findings in order to prove that the optimized performance has been achieved.



## **1.4 Scope and Limitation**

This thesis mainly involves the design of simulation of an air-filled SIW circuit together with the dielectric- to air-filled transition which is able to operate in high-quality microwave and millimeter wave integrated circuits and systems. The transition is designed for the Roger RT/Duroid 6002 substrate in the Ka-band frequencies (26 – 40 GHz) and U-band frequencies (40 – 60 GHz). The transition taper is designed with various geometrical functions such as linear, parabolic, exponential, and raised cosine tapers. To further minimize the losses of the transition, the combination of cubic clamped spline function and the genetic algorithm method is used to find an optimal transition design. The S-parameters results by full-wave analysis of the transition with varying geometry are exported in the form of Excell and all graphs are compared. For the optimization method, the optimization procedure is developed in this thesis.

## **1.5 Thesis Outline**

This thesis consists of six chapters. The first chapter gives the background of a waveguide, SIW, air-filled SIW, dielectric- to air-filled SIW transition and analyses that are required to be conducted. Besides, the other elements such as the problem statements, the objectives, the scope and the outline of the thesis are included. In chapter two, a literature review regarding of an air-filled SIW, dielectric- to air-filled SIW transition, designed shape of the transition taper, losses of the transition, the clamped cubic spline method and optimization procedure will be presented. The theories of the inhomogeneous waveguide, as well as an air-filled SIW transition, are presented in chapter three.

The numerical approach and methodology used to perform full-wave analysis of the dielectric- to air-filled SIW transition are introduced in chapter four. Additionally, the optimization procedure, design specifications, flowchart, software required and detailed description of project flow will be described in this chapter. Results from chapter four are presented and discussed in chapter five. Finally, the thesis will be ended with conclusions in chapter six.

## CHAPTER TWO

### LITERATURE REVIEW

In Chapter 1, the goal of this thesis is to understand the return and transmission losses along the transition in an air-filled SIW circuit in order to completely characterize the losses in an air-filled SIW complete structure. Another goal is to optimize losses in an air-filled SIW complete structure. Accordingly, the full-wave analysis of an air-filled SIW structure is emphasized to characterize the losses. Furthermore, the topology of the tapered transition of the dielectric- to air-filled SIW transition is designed with various geometrical functions to evaluate the transition losses. Additionally, an optimization procedure is developed to further minimize the losses.

In this chapter, details method to calculate the eigenvalues of the inhomogeneous waveguide are discussed because it can effectively imitate an air-filled SIW. The details of SIW and air-filled SIW structure are presented where the contribution of the previous research is stated. The previous researches on dielectric- to air-filled SIW transition and non-uniform circular waveguide transition are also discussed. Besides, the optimization procedure based on genetic algorithm is elaborated. Finally, the clamped cubic spline method is described.

#### **2.1 Inhomogeneous Waveguide**

As mentioned in Chapter 1, an air-filled SIW structure is more complex as an inhomogeneous waveguide. In general, any waveguide filled with two or more

different material composition is known as an inhomogeneous waveguide. For the past few years, these waveguides have received considerable attention because of their application in a variety of waveguide components. In microwave engineering, the inhomogeneous rectangular waveguide has been widely used as transmission line due to its low insertion and high power capability compared to the conventional waveguide.

As a result, the analysis of these waveguide has been the subject of a number of research works over the last two decades. A complete theoretical analysis of the dielectric loaded rectangular waveguide has been illustrated in Vartanian et al. (1957) and Seckelmann (1966). The calculation of eigenvalues including propagation constants and cut off wavelengths are calculated by solving the characteristic equations containing transcendental functions i.e., a function that cannot be described with polynomials (Vartanian et al., 1957). However, the calculation of eigenvalues becomes difficult because of the transcendental equations were involved.

Therefore, numerical methods are used instead by some researchers to solve the eigenvalue problem in a dielectric loaded waveguide. For example, a variational method is used in Collins (1960) and Yu and Chu (1990). The finite element method has been applied by Azizurn and Davies (1984) and Nuno et al. (1997). Silvestre et al. (2000) presented the bi-orthonormal-basis method to analyze inhomogeneously filled waveguides with lossy dielectrics. According to Yu and Chu (1990), other numerical methods such as the variation, finite element, mode-matching, variation-iteration and hypergeometric functions are efficient for calculating eigenvalues of the fundamental mode. On the other hand, for the complex geometry of inhomogeneous waveguide that had no analytical solutions, the numerical approaches must be

applied to solve the guided wave problems. For example, the radially inhomogeneous circular dielectric waveguide problem was solved in Dil and Blok (1973) using the numerical integration technique.

Besides, the finite element method of an arbitrarily shaped inhomogeneous optical fiber has been reported in Yeh et al. (1975). Yeah and Shimabukuro (2008) showed that the other complex geometry of inhomogeneous guided wave problems can be solved by applying numerical techniques such as the finite element, finite difference, and beam propagation method. Furthermore, accessibility of computing power encouraged rapid adaptation of numerical techniques to solve electromagnetic problems, resulting in the commercialization of computer programs based on the numerical techniques (Yeh and Shimabukuro, 2008).

## **2.2 Air-Filled Substrate Integrated Waveguide**

One of the examples of the inhomogeneous waveguide with a complex geometry is an air-filled SIW. This type of waveguide is developed from the modification of SIW. In microwave engineering, there is an increasing demand for developing high-quality microwave and millimeter wave integrated circuits and system. Therefore, a waveguide device is used for the design of microwave circuits rather than the transmission line as at high-frequency, transmission lines become inefficient as a result of skin effect and dielectric losses (Cheng, 1989). However, they are bulky and non-planar in nature (Kumar et al., 2012). Thus, it is difficult to integrate and to manufacture at low cost in the planar structure. Therefore, a synthetic rectangular metallic waveguide filled with dielectric material is constructed in planar form, thus allowing a complete integration with other planar transmission-

line circuits (Shigeki, 1994). The post-wall waveguide has later been proposed by Hirokawa and Ando (1998) and laminated waveguide introduced in Uchimura et al. (1998).

Later on, waveguide-like structures called SIW that can be fabricated in planar circuits by using two periodic metallic vias holes was proposed by Deslandes and Wu (2001). As shown in Figure 2.1, the sidewalls of the rectangular waveguide can be realized within the substrate by using a metalized array of vias or a metalized groove technique. SIW is a transition between microstrip and dielectric-filled waveguide (DFW). DFW is converted to SIW with the help of vias for the side walls of the waveguide and due to the existence of vias at the sidewalls, transverse electric (TE) modes exist only and the dominant mode will be  $TE_{10}$ .

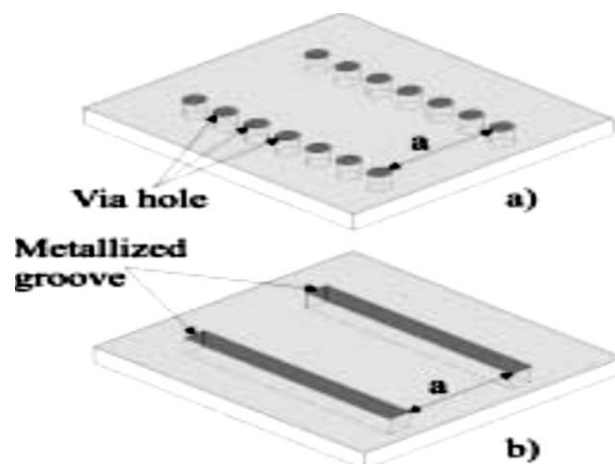


Figure 2.1: Substrate integrated waveguide: a) metalized via holes arrays b) metalized grooves. (Deslandes and Wu, 2001).

Nowadays, various methods to design SIW have been proposed. Each method uses different materials as substrates and geometry of metallic vias as well as approaches to find the appropriate parameters. For example, the earliest design technique for SIW was reported in Deslandes and Wu (2001). After that, the more details design technique and analysis of SIW has been presented in Deslandes and

Wu (2006). Ng (2014) has proposed the metal via-holes of the square and rectangular cross-section in the implementation of SIWs as illustrated in Figure 2.2. Furthermore, another design technique for SIW has been presented in Kumar et al. (2012) and Bozzi et al. (2009) as described in Figure 2.3.

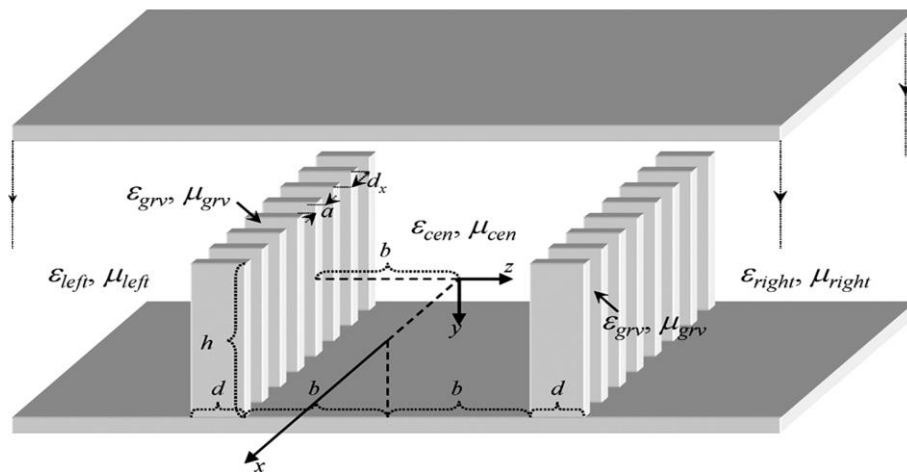


Figure 2.2: Schematic and geometry of SIW (Ng, 2014).

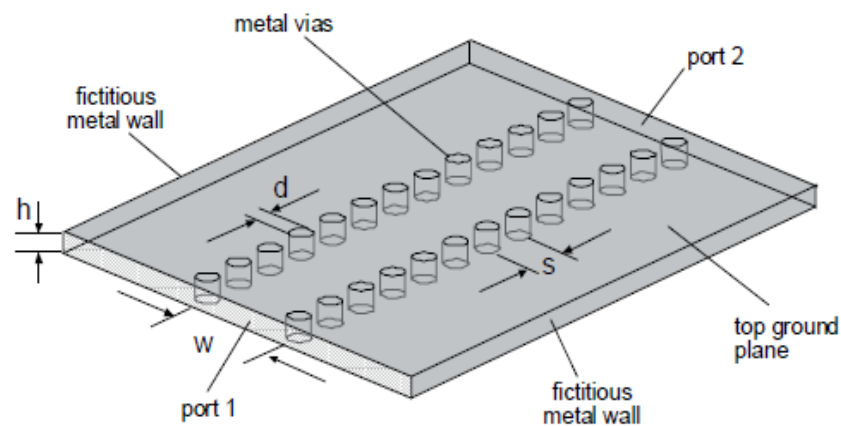


Figure 2.3: Substrate integrated waveguide (Bozzi et al., 2009).

The full-wave analysis of SIW based on numerical methods to understand the mechanism in SIW has been done in previous research. Xu and Wu (2005) studied the guided wave, modes characteristic and providing basic design rules of SIW in details. Moreover, the dispersion characteristic of SIW and it's designed method is obtained in Cassivi et al. (2002). The full-wave analysis of SIW also has been

presented in Xu et al. (2003) and Xu et al. (2005). The equivalent circuit models of SIW discontinuities and full-wave analysis for the direct determination of multi-mode equivalent circuits for SIW discontinuities has been proposed in Bozzi et al. (2006).

Wu et al. (2003) then introduced the substrate integrated circuit (SIC) concept and this led to intense worldwide research activity into the SIW and its applications. Since that, a large variety of SIW components, such as filters, antennas, transitions, couplers, power dividers, and oscillators, have been proposed and implemented for operation in the microwave and mm-wave range (Bozzi et al., 2009).

The advantages of SIW technology are the possibility to fabricate a complete circuit in a planar form such as including planar circuitry, transitions, rectangular waveguides, active components, and antennas, using a standard printed circuit board or other planar processing techniques. Furthermore, the SIW component structures also maintain most of the advantages of conventional metallic waveguides, such as complete shielding, high quality-factor, and high power-handling capability.

However, one of the major issues in the design of SIW components is related to the minimization of the losses. Bozzi et al. (2009) have reported that the dielectric loss is typically the most significant contribution to losses in the mm-wave frequency range.

Therefore, a significant effort has been devoted to the research and development of low loss SIW in the last few years. As an example, the half-mode substrate integrated waveguide (SIW) introduced by Li et al. (2009) where the waveguide width and the surface area of the metallic sheets are reduced by nearly



half compared with the SIW as depicted in Figure 2.4.

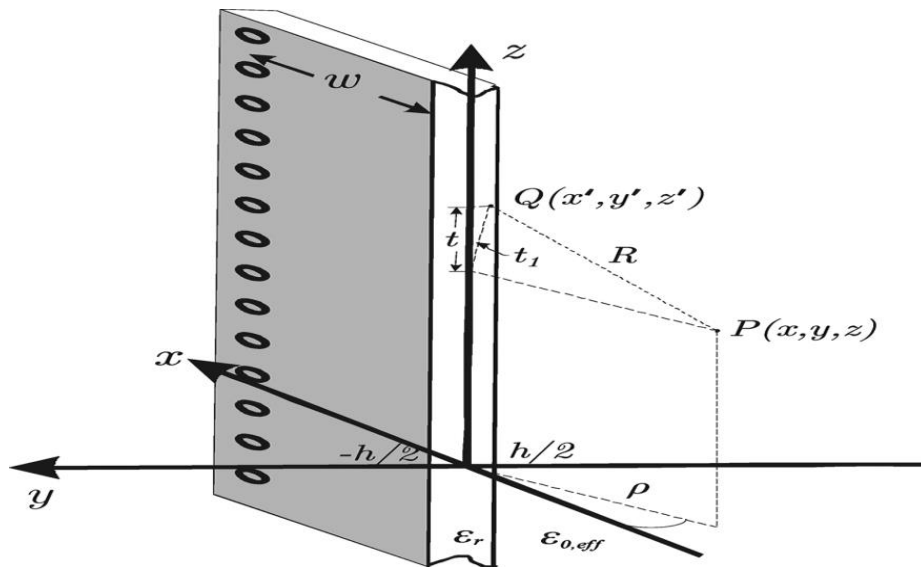


Figure 2.4: Half-mode substrate integrated waveguide (Lai et al., 2009).

Since then, there are several theories and design that has been attempted by removing the central dielectric region of an SIW with the intention to reduce the dielectric loss and to achieve a lower loss. Modified SIW with an air cut region as shown in Figure 2.5 has been introduced by Ranjkesh and Shahabadi (2008) where a computational analysis of the attenuation constant and cutoff frequency are reported. The attenuation constant of the SIW caused by dielectric loss can be reduced significantly by increasing the  $w/a$  ratio, where  $w$  is the width of the air-cut region and  $a$  is the width of the SIW.

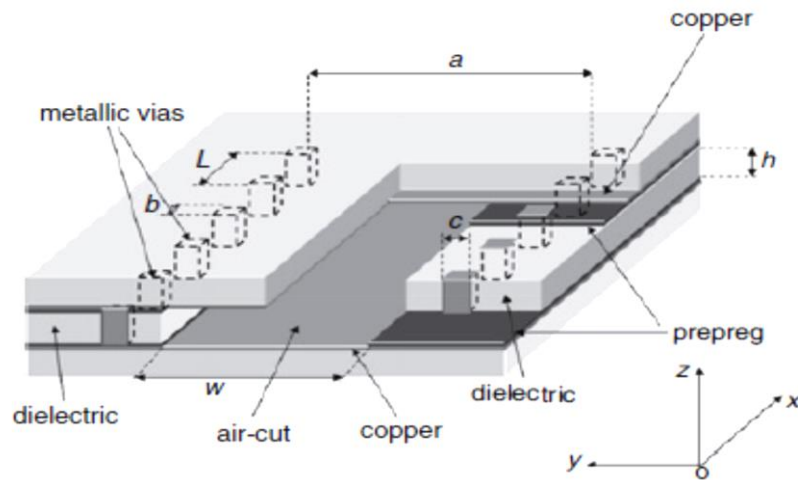


Figure 2.5: Modified substrate integrated waveguide (Ranjesh and Shahabadi, 2008).

Furthermore, Hollow Substrate Integrated Waveguide (HSIW) has been presented in Jin et al. (2014). Recently, the attractive feature of an air-filled SIW as shown in Figure 2.6 has been theoretically and experimentally demonstrated in Parment et al. (2015).

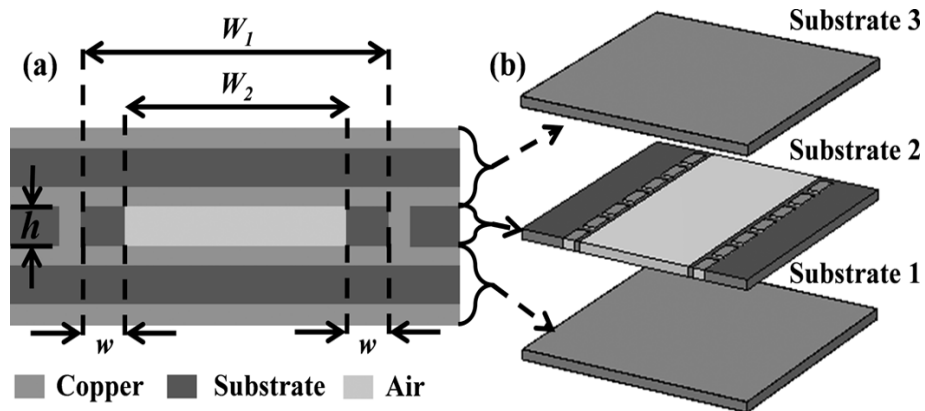


Figure 2.6: Air-filled substrate integrated waveguide (Parment et al., 2015).

The theoretical and analysis results of the proposed structure showed a significant improvement in terms of losses and power handling capabilities as compared to the conventional dielectric-filled SIW (Parment et al., 2015). As a result, an air-filled SIW structure can be used for the design of more complex passive

circuits. A transition allowing interconnection of an air-filled with the dielectric-filled SIW has been reported in Parment et al. (2015). Another attempt using a similar approach of having an air-filled region with tapered transitions is introduced in Belenguer et al. (2014), where the empty substrate integrated waveguide (ESIW) has been proposed.

### **2.2.1 Air-Filled SIW Structures**

One of the approaches in fabricating an air-filled SIW is the removal of the central region of the dielectric substrate between the periodic metallic vias of the SIW, thus creating a hollow region between the two arrays of metallic vias. An improved construction is based on a multilayer Printed Circuit Board (PCB) process, where layers of the substrate were added on the top and bottom of an air-filled SIW to act as conducting boundaries as depicted in Figure 2.6.

The transmission medium of the structure is composed of a combination of air and dielectric material. The equivalent RW of SIW is a well-acknowledged method for modeling the SIW and has been presented in Che et al. (2008). An air-filled SIW owing to the inhomogeneity introduced by the air-cut inside the structure has been referred in Ranjkesh and Shahabadi (2006). As a consequent, it can be modeled as inhomogeneous rectangular waveguides because of the inhomogeneity introduced by the air-region in the middle of the structure.

The theoretical analysis of inhomogeneous rectangular waveguide is used for analyzing an air-filled SIW by Parment et al. (2015). Based on the structure proposed in Parment et al. (2015) the geometry parameters of an air-filled SIW structure can

be calculated from the characteristic equation of inhomogeneous rectangular waveguide obtained from Vartanian et al. (1957) as equation (2.1)

$$\tan\left(\frac{\sqrt{\varepsilon_r}(W_1 - W_2)\pi f_c}{c}\right) = \sqrt{\varepsilon_r} \cot\left(\frac{W_2\pi f_c}{c}\right), \quad (2.1)$$

where

- $c$  = velocity of the light,
- $\varepsilon_r$  = substrate permittivity,
- $f_c$  = cut off frequency,
- $W_1$  = total width,
- $W_2$  = width of the air-filled region respectively, such that  $W_1 - W_2 = 2w$ .

### 2.2.2 Dielectric- to Air-Filled SIW Transition

To allow an effective interconnection of dielectric- to air-filled SIW circuits, a transition as depicted in Figure 2.7 is proposed in Parment et al. (2015). The transition consists of air- and dielectric-filled that is tapered from air-filled SIW into SIW.

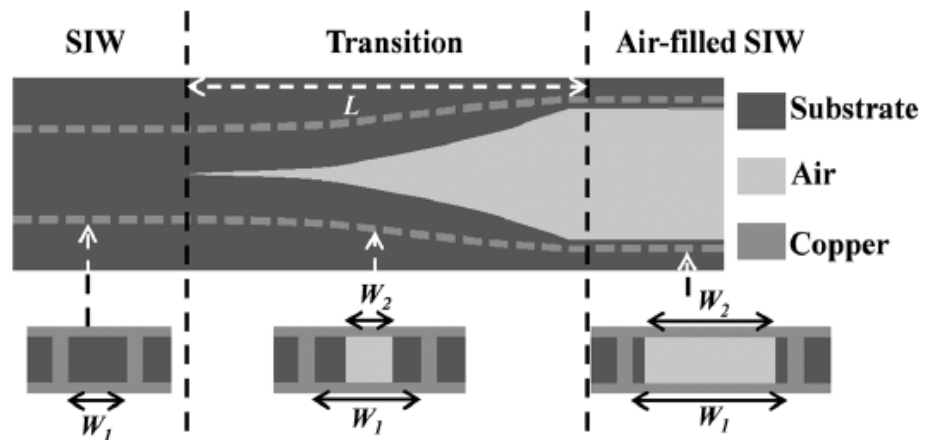


Figure 2.7: Air-filled SIW transition (Parment et al., 2015).

Based on the theoretical theory in Kraus and Fleisch (1999), as a wave incident normally between two different media with intrinsic impedances, part of the incident wave is reflected back while another part is transmitted into the second medium. To overcome this problem a  $\frac{\lambda}{4}$  thickness of one dielectric can be used to match the incident space wave into half space of another dielectric to reduce the reflected wave and increase transmitted wave (Kraus and Fleisch, 1999). Kraus and Fleisch (1999) indicated that a pyramid matches the wave analogous to a tapered transmission line and results in a low reflected loss.

According to Ghassami et al. (2014), the development of a wideband transition of the transmission line on a different dielectric constant substrate becomes critical for complete front-end integration and low-cost system manufacturing. Hence a wideband low-loss integrated transition of SIW on high-to-low dielectric constant substrates was designed by optimizing the length and width of the transition taper (Ghassami et al., 2014). Furthermore, any low-loss, transition design required can be designed by optimizing the structural parameters of the transition design. As an example, when the geometrical dimensions of the transition taper on high-to-low dielectric are optimized, the transition losses are minimized as reported in Belenguer et al. (2014).

Back to air-filled SIW transition, the design of the taper for the transition on dielectric-to air-filled SIW using the characteristic equation has been shown to be effective in Parment et al. (2015). To improve the performance of an air-filled SIW circuit, the transition from the dielectric substrate toward the hollow, i.e., the air-filled region must be properly characterized (Parment et al., 2015). From the full-wave analysis results presented in Parment et al. (2015) an increment of the

transition length caused wide bandwidth of lower return loss and increased the transmission loss. This leads to a trade-off between total transition length and losses.

In addition, an air-filled SIW transition is a non-uniform waveguide transition structure as shown in Figure 2.7. This is because each SIW is dimensioned for operating in the fundamental  $TE_{10}$  mode. The problem of a non-uniform waveguide transition is its losses. As a result, the relationship of a non-uniform circular waveguide transition length and taper design on transition losses has been presented in Hecken (1972) and Hecken (1973). Furthermore, based on the optimization procedures in Nagarkoti et al. (2012), it was found that the raised cosine shape profile nonlinear taper is an optimal shape of transition since it has minimal shaper variation at both ends thereby ensuring minimal reflections.

Moreover, to reduce the loss of a circular waveguide taper, the geometry of the transition taper is optimized with various equations for taper such as exponential, parabola, linear and raised cosine function in Donda et al. (2015). Despite return and transmission loss, the major problem with circular waveguide tapers is mode conversion loss and spurious modes which are unwanted modes converted by power. In fact, the raised cosine profile of circular waveguide taper which had very low mode conversion has already been presented by Unger (1958) and by using the Fourier transform of Tschebycheff polynomial the design of the raised cosine circular waveguide taper was developed.

### **2.3 Optimization Procedure**

To create a new design of an air-filled SIW transition with a lower loss over wide-bandwidth, the design of the transition taper of an air-filled SIW transition is

optimized in this thesis, where an optimization procedure is developed. In engineering design, the process of determining the best design is called optimization. As stated in Rao (2009), the ultimate goal of all such decisions is either to minimize the effort required or to maximize the desired benefit. Since the effort required or the benefit desired in any practical situation can be expressed as a function of certain decision variables, optimization can be defined as the process of finding the conditions that give the maximum or minimum value of a function. An optimization problem can be summarized as follows (Rao, 2009)

$$\text{Find } X = \left\{ \begin{array}{c} x_1 \\ x_2 \\ \vdots \\ x_n \end{array} \right\} \text{ which minimizes } F(X)$$

This value is subject to the constraints outlined below

$$G_j(X) \leq 0 \text{ for } j = 1, \dots, m$$

$$L_j(X) = 0 \text{ for } j = 1, \dots, p$$

the variable  $X$  is called the design vector and  $F(X)$  is the objective function. Where  $G_j(X)$  and  $L_j(X)$  are known as inequality and equality constraints. The problem stated above is called a constrained optimization problem. For optimization, a problem which does not involve any constraints is called unconstrained optimization problems. For a single-objective optimization problem, assuming minimization, if  $F(X)$  is a scalar value the optimization goal is to minimize this value. Multi-objective optimization however,  $F(X)$  is a vector of objectives that means it is a multi-objective optimization problem. The optimization goal is to minimize all the objective functions simultaneously.

There are various methods introduced by previous researchers for solving different types of optimization problems. Recently, the modern optimization methods have emerged as powerful and popular methods for solving complex engineering optimization problems. These methods include genetic algorithms, simulated annealing, particle swarm optimization, ant colony optimization, neural network-based optimization, and fuzzy optimization detailed in Rao (2009).

Among others, a genetic algorithm (GA) is widely used in engineering design for its efficiencies, adaptivity, and robust search and optimization processes. Besides, GA uses guided random choice as a tool for guiding the search in very large, complex, and multimodal search spaces (Bandyopadhyay and Saha, 2013). GA is a popular in electromagnetic engineering due to the fact that it is robust and based on stochastic-based search methods, which can handle the common characteristics of electromagnetic optimization problems that are not readily handled by other optimization methods such as simulated annealing, particle swarm optimization, ant colony optimization, neural network-based optimization, and fuzzy optimization (Johnson and Rahmat-Samii, 1997). Moreover, they are particularly effective to find an approximate globe maximum in a high-dimension, multimodal function in a near-optimal manner (Rahmat and Michielssen, 1999).

Furthermore, a lot of practical optimum design problems are characterized by mixed continuous-discrete variables, discontinuous and nonconvex design spaces. If standard nonlinear programming techniques are used for this type of problem they will be inefficient, computationally expensive, and, in most cases, find a relative optimum that is closest to the starting point. Therefore, GA is well suited for solving such problems, and in most cases, it can find the global optimum solution with a



higher probability (Rao, 2009).

Design using the GA in engineering electromagnetic has been widely used such as design of a microstrip antenna in Choo and Ling (2003), a magnetizer in Fuat Uler et al. (1995), thinning linear and planar arrays in Haupt (1994) and design of lightweight, broadband microwave absorbers in Michielssen et al. (1993) etc. As stated by Johnson and Rahmat-Samii (1997), the electromagnetic optimization problems generally involve a large number of parameters and those making the design process inefficient and difficult. The combining of full-wave electromagnetic simulation software with optimization methods is a promising technique. In this thesis, the optimization procedures of an air-filled SIW transition based on the combination of GA with the ANSYS HFSS will be developed.

### **2.3.1 Single-objective Genetic Algorithm**

Genetic algorithms are powerful and robust stochastic search and optimization techniques, which have been applied to many engineering and mathematical areas such as engineering design. They are originally designed for single-objective optimization problem and they used a fitness function to perform an evaluation. Genetic algorithms are global optimization techniques that are based on the mechanism of the Darwinian theory of natural selection and evolution. Genetic algorithms offer many advantages compared to traditional numerical optimization techniques including the ability to use both continuous and discrete parameters, search across a wide sampling of the solution space, and could handle a large number

of variables. GA steps are described as follows (Rao, 2009):

1. Initialize a random population of chromosomes.
2. Compute the fitness of each population member.
3. Rank the individuals based on fitness.
4. Generate offspring by mating good individuals.
5. Mutate selected members of the offspring.
6. Stop if conditions have been met or continue back to step 2.

### **2.3.2 Multi-objective Genetic Algorithm**

Over the past decade, genetic algorithms have been extensively applied to multi-objective optimization problems. As mentioned in section 2.2.2, the increment of transition length causes the wide bandwidth of return loss and increment of transmission losses. In order to further minimize the losses, the design of the air-filled SIW transition is needed to optimize. The transition losses consist of transmission and reflection losses. With regard to that matter, the third objective of this thesis is to develop an optimization procedure using the multi-objective genetic algorithm.

As stated in Deb (2001), the presence of multiple conflicting objectives is natural in many problems and this makes the optimization problem interesting to solve. The author concluded that no single solution can be taken as an optimal solution to multiple conflicting objectives, the resulting multi-objective optimization problem resorts to a number of trade-off optimal solutions. Thus, the multi-objective optimization method will be practiced in this study.

Deb (2001) summarized that the multi-objective problem, gives rise to a set of optimal solutions as known as Pareto-optimal solutions, instead of a single optimal solution. In the absence of any further information, one of these Pareto-optimal solutions cannot be said to be better than the other. This demands a user to find as many Pareto-optimal solutions as possible. Hence the Pareto-based techniques are utilized. The primary reason for this is the ability of GA to find multiple Pareto-optimal solutions. Since the genetic algorithm (GA) worked with a population of solutions, a simple GA can be extended to maintain a diverse set of solutions. With an emphasis on moving toward the true Pareto-optimal region, GA can be used to find multiple Pareto-optimal solutions in one single simulation run.

The multi-objective GA works on a population using a set of operators that are applied to the population. A population is a set of points in the design space. The initial population is generated randomly. The next generation of the population is computed using the non-dominated rank and a distance measure of the individuals in the current generation. The multi-objective GA function uses a controlled elitist genetic algorithm. An elitist GA has always favored individuals with better fitness value (rank) whereas, a controlled elitist GA also favors individuals that can help increase the diversity of the population even if they have a lower fitness value.

It is very important to maintain the diversity of population for convergence to an optimal Pareto front. This is managed by controlling the elite members of the population as the algorithm progresses. There are different approaches of a controlled elitist genetic algorithm such as Niche Pareto GA (NPGA) by Horn et al. (1994), Non-dominated sorting GA (NSGA) by Srinivas and Deb (1995) and Strength Pareto evolutionary algorithm (SPEA) in Knowles and Corne (1999) with